Malaysian Journal of Catalysis
http://mjcat.utm.my/
MJCat

The effect of RF-sputtering temperature of Yittria-Stabilized Zirconia nanostructure electrolyte for SOFC application

S.Y. Jaffar[a], Y.Wahab[a], R.Muhammad[b], Z.Othaman[b], S. Sakrani[b], Z. Ibrahim[b]
[a]*Razak School of Engineering and Advanced Technology, Universiti Teknologi Malaysia,54100 jalan Yahya Putra(Semarak), Kuala Lumpur, Malaysia.*
[b]*Department of Physics, Faculty of Science, Universiti Teknologi Malaysia, 81310 UTM Johor Bahru, Johor, Malaysia*
**Corresponding author email:* yasminchang11@gmail.com

Article history :
Received 1 September 2016
Accepted 21 August 2017

GRAPICAL ABSTRACT

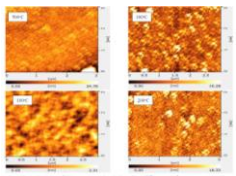

ABSTRACT

Yttria-stabilized zirconia (YSZ) thin films were fabricated successfully using reactive RF magnetron sputtering. The substrate had been used are sapphire glass. A pure ceramic of Zr-Y is synthesized and processed into a planar magnetron target which is reactively sputtered with an Argon-Oxygen gas mixture to form Zr-Y-O nanostructure. The aim of this research is to synthesize YSZ thin film by using RF magnetron sputtering by varying the temperature deposition parameter. In this work, this research is to study the structural, morphological, thickness of YSZ nanostructure that can be used as electrolyte for solid oxide fuel cell (SOFC). By lowering the YSZ thin film into nanostructure would enable for SOFC to be operate at lower temperature below 400 ºC. The YSZ nanostructure were controlled by varying the deposition parameters, including the deposition temperature and the substrate used. The crystalline of YSZ structure at 100W and temperature 300 ºC. X-ray diffraction study revealed that the optimum peak obtained for YSZ thin film at (111) and (002). The surface morphology of the films proved that at 300oC temperature rate deposition showed optimum growth morphology and density of YSZ thin films. Besides, the high deposition time affected the thickness of YSZ thin film at 80nm by using surface profiler. A higher rate of deposition is achievable when the sputtering mode of the Zr-Y target is metallic as opposed to oxide. YSZ is synthesizing to obtain the optimum thin film for SOFC application.

Keywords: RF magnetron sputtering, electrolyte, SOFC, YSZ, RF-sputtering power.

1. INTRODUCTION

Solid oxide fuel cell (SOFC) technology, which offers many advantages over traditional energy conversion systems including low emission and high efficiency, has become increasingly attractive to the utility, automotive, and defense industries. As an all solid-state energy conversion device, the SOFC operates at high temperatures (700-1,000 ºC) and produces electricity by electrochemically combining the fuel and oxidant gases across an ionically conducting oxide membrane. Yttria stabilized zirconia (YSZ) is the most commonly used material for solid oxide fuel cell (SOFC) electrolytes [1] as it is an adequate ionic conductor, has a low electronic conductivity, and is relatively cheap to process compared to other electrolyte materials. The ionic conductivity in the stabilized zirconia system is due to the mobility of O^{2-} vacancies created when substituting Zr^{4+} by Y^{3+} in the cationic network. However, the ionic conductivity of state-of-the-art YSZ based electrolytes is only sufficient at elevated temperatures (800-1000 °C) which results in increased reactivity of cell core components, drastically limited lifetimes and requires the use of expensive interconnect materials [2]. Therefore, the reduction of the operation temperature to an intermediate temperature range (200-300 °C) is a key objective in SOFC research. Among the possible routes to achieving lower operation temperatures, reduction of the electrolyte thickness in order to reduce the overall resistance is promising [3-4].

YSZ electrolytes are typically fabricated by screen printing or spraying techniques followed by subsequent sintering [5] which are ideal for low-cost fabrication with high throughput. However, these methods are not suitable for producing dense and thin (a few μm in thickness) YSZ electrolytes. The latter can be achieved by synthesizing YSZ thin films employing a variety of chemical and physical methods [6] such as pulsed laser ablation (PLD), chemical vapor deposition (CVD) [7], atomic layer deposition (ALD) [8], spin coating [9] and magnetron sputtering [10,11,12]. An issue often encountered when depositing YSZ thin films by physical vapor deposition techniques (PVD) for example magnetron sputtering at relatively low synthesis temperatures is the formation of undersense and columnar microstructures. Such microstructures are unfavorable as they may result in internal leakage in the cell leading to decreased open cell potential. Therefore, an undesirable extra manufacturing step in the form of post-deposition annealing is often required to eliminate pores in such films [13]. Reports on cell tests performed on SOFCs containing magnetron sputtered electrolytes with a columnar structure have shown an electrochemical performance comparable to or worse than cells containing tape cast electrolytes and not a significant improvement as would be expected from the reduced electrolyte thickness [14]. This lack of performance is related to leaks in the electrolyte due to the columnar morphology. In contrast, Nédélec et al. have deposited electrolytes without visible continuous columnar structure and has achieved

significant improved electrochemical performance at low temperatures [15].

2. MATERIALS AND METHODS

2.1 Methodology

The substrate cleaning is very important in the deposition on thin films. A glass with a size of 2 cm x 2 cm was cut. Then, the glass slides were placed in beaker filled with acetone and the beaker was put into Power Sonic405 for 10 minutes. After that the acetone was replaced with water and again, put the beaker into Power Sonic405 for 3 minutes. This step was repeated for 3 times. Finally, the glasses were dry using nitrogen gas or oven with the time was set for 10 minutes at temperature 100°C.

Yttria-stabilized zirconia (YSZ) thin films were deposited on soda lime glass by RF magnetron sputtering technique using an Advanced Energy Cesar 1.36 generator operating at 13.56 MHz coupled with a 25.4 mm Angstrom circular magnetron mounted on a standard DN 400 KF recipient. Commercial YSZ powders, 8 mol% Y_2O_3 99.9% purity TOSOH Inc. Japan. Before each process the deposition chamber was pumped down to 4×10^{-6} mbar, while during deposition a pressure of 3.8×10^{-6} mbar was obtained introducing Ar and O_2 in the ratio PO_2/PAr =0:1. The RF-power used was 100W which, with a target-substrate distance of 10cm, allowed a deposition rate of 2 nm/min. The substrate temperature during deposition was varied from room temperature until 450◦C as recorded by a thermocouple embedded in the sample holder stage.

2.2 Characterizations

The film thicknesses were analysed by surface profiler and scanning electron microscopy (SEM) using a Dektak 8 system and a Zeiss Supra VP55, respectively. Grain size distributions were obtained from top view scanning electron microscopy (SEM) images by the Heyn's mean lineal intercept method [33], measuring at least 500 individual grains. Rutherford backscattering spectroscopy (RBS) and particle-induced X-ray emission (PIXE) using 2 MeV 4He ions and 3 MeV protons as projectiles provided information on the chemical composition of the films. In order to study the crystallization of the 8 mol%-YSZ thin films, the deposited samples were annealed in air at different temperatures between 28 and 450 °C for dwell times from 1 min to 85 h. The as-deposited and annealed samples were analysed with X-ray diffraction (XRD) using a Bruker D8 Advance diffractometer with a Copper anode and a Ni-filter. For the analysis of the crystallinity, because of the limited number of diffraction peaks and the strong texture observed, only (111) peak of the YSZ film was fitted with a pseudo-Voigt function using the FIT software [16], from which the integrated peak area A(t) and the integral breadth β(2θ) of the peak were determined. The volume weighted average diameter of crystalline grains D and microstrain ε were determined from the integral breadths of the Lorentzian and Gaussian components of the pseudo-Voigt function, respectively βL and βG, as described in Ref. [17]:

$$D = \frac{K_\beta \lambda}{\beta_L Cos\theta} \quad (1)$$

$$\varepsilon = \frac{\beta_G}{4\tan(\theta)} \quad (2)$$

where Kβ is the Scherrer constant, which for (hh0) reflexes and cubic shape is)[18].

3. RESULTS AND DISCUSSION

3.1 Effect on RF-sputtering power

The XRD θ − 2θ patterns of YSZ thin films deposited at different sputtering temperature from 28◦C to 400 ◦C but for the same O2: Ar ratio (0.1) are shown in Fig.1. It is found that the orientation of YSZ film is not sensitive to sputtering power. Only YSZ (111) peaks are detected in a large power range of 50 W–150 W. The other peaks are from the substrates. The intensities of YSZ (111) films are almost similar in the semi-log scale plots. However, careful observation of YSZ (111) peaks from 30° to 55° shows that the YSZ (111) peaks first shift to higher 2θ, then shift to lower 2θ, at last shift to higher 2θ again. The intensity of YSZ (111) peak increases with increasing the sputtering temperature, which indicates that the YSZ films become thicker with increasing the sputtering power.

The YSZ (111) peak position shifting indicates a variation in lattice spacing with enhancing sputtering power. It implies the change of stress for the YSZ films. As the sputtering temperature increases, the thickness of YSZ film becomes thicker for the same sputtering time. Hence, the peak shift phenomenon can be explained by a thickness dependency of stress mechanism. This stress development on thickness may arise from thermal stress or intrinsic stress. In our case, all YSZ films are fabricated at the same temperature with the same coefficient of thermal expansion and elastic modulus. Therefore, it is believed that the stress origins from intrinsic stress not thermal stress.

Table 1 FWHM and grain size YSZ nanostructure

Power deposition	Crystallographic (HKL)	FWHM	Grain size (nm)
100W	(002)	0.1349	20.5
100W	(111)	0.1268	21.6
150W	(002)	0.1133	24.2
150W	(111)	0.2838	26.6

As the temperature from 28◦C to 400◦C the peak position of the YSZ (111) shifts to higher 2θ, which is believed to origin from the tensile stresses in the YSZ films. And the stress will release gradually as the film thickness approaches to a certain value. For the film deposited at 150 W, the peak site of YSZ (111) shifts to lower 2θ compared to the film deposited at 100 W. It is suggested that the tensile

stress emerges again. The second time appearance of tensile stress has been reported several times for (Re) BCO films [18, 19]. It is believed that surface roughness [20], the oxygen vacancies [21] and tilted grains [22] can be the reasons of this phenomenon. The peak site of YSZ (111) shifts to higher 2θ for the film fabricated with temperature 300oC, which indicates the decrease of tensile stress for the film. Fig. 3 is the AFM images of YSZ films deposited with the same O_2: Ar ratio (0.1) but different sputtering power from 50W to 150W. Although the orientation of YSZ film is sensitive to sputtering power, the values of roughness and grain size for YSZ films are obviously affected by the sputtering power. The smaller grain size of 2–3 nm is obtained for the YSZ film deposited with low sputtering power 50W. The grain size increases as the sputtering power increases. When the sputtering power increases to 150 W, the average grain size increases to 26.6 nm. The surface roughness is strongly depended on the grain size. The surface is rather smooth with a RMS value of 0.6 nm for YSZ film deposited at 100 W. With enhancing sputtering power from 50W to 150W, the RMS value increases to 6.1 nm. Many aspects can affect the development of the surface morphology, such as adsorption, nucleation and island forming. Recently, an islands growth model is proposed by Bartelt *et al*. [23]. In this model, the island size depends on two parameters. One is the deposition rate r, which is mainly determined by sputtering power. The other one is the diffusion rate h_0, which is mainly determined by growth temperature. Then, the D determines the island size distribution. The island density N is a very important parameter for irreversible island formation. In Bartelt *et al'* model [23], as the ratio D increases, deposited atom can travel farther. So the island density N decreases with enhancing the ratio D. As to our cause, it is evident that the deposition rate is higher with higher sputtering power. The diffusion rate h_0 is the same because of the same deposition temperature. As the sputtering power increases, the ratio decreases. This leads to the increasing of the island density N. In addition, more and more islands appear on the full covered surface, as shown in Fig. 2. This leads to bigger grain size with 40 nm. As a result, the grains with the biggest size 50 nm appear for the highest sputtering power of 150W, as shown in Fig. 3(a). The roughness of YSZ film is associated with the values of peaks and valleys of film surface. The line profiles of deposited YSZ films are shown in Fig. 5. With lower sputtering power, the average value of peaks and valleys is less than 1 nm, as shown in Fig. 3(c). With increasing the sputtering power from 50 W to 150 W, the average value of peaks and valleys increases from 2.0 nm to more than 3.6 nm. With lower sputtering power, few atoms arrived at the surface at the same time. Hence, they can escape from island edges to fill valleys. This causes the flat surface. With higher sputtering power, more atoms arrived at the surface at the same time. Therefore, they can't escape from island, which will enhance the values of peaks. It results in rough surface.

The above discussion is related to the decrease of surface diffusion effects, which usually lead to a slower roughness increasing. It is noted that with power increasing from 50 W to 150 W, the film surface roughness increases slowly. However, when the power reaches 150 W, there is an abrupt increase of film roughness. The abrupt increase of film roughness cannot be simply explained by the decrease of surface diffusion effects.

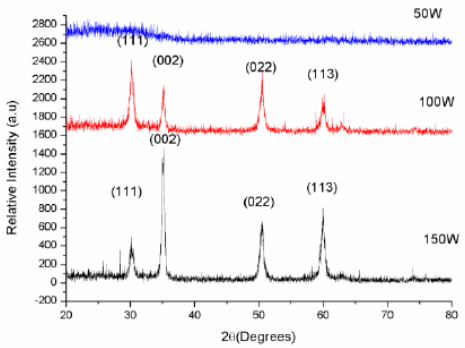

Fig. 1 XRD θ − 2θ patterns of YSZ films deposited with sputtering power from 50W until 150W from 20° to 60∘

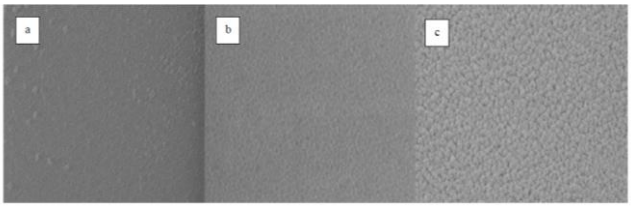

Fig. 2 FESEM images of YSZ nanostructure deposited on Al2O3 at different power from 50W to 150W.

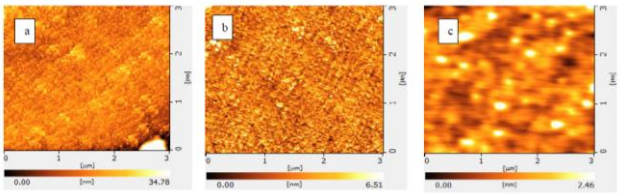

Fig. 3 AFM images of YSZ nanostructure deposited on Al2O3 at different power from 50W to 150W.

3.2 Effect on susbtrate temperature

The XRD θ − 2θ patterns of YSZ thin films deposited at different sputtering temperature from 100oC to 500oC but for the same O2: Ar ratio (0.1) are shown in Fig.1. It is found that the orientation of YSZ film is sensitive to sputtering substrate temperature. Only YSZ (111) and (002) peaks are detected in a large substrate temperature range of 100oC to 500oC. The other peaks are from the substrates. The intensities of YSZ (111) films are almost similar in the semi-log scale plots. However, careful observation of YSZ (111) peaks from 30° to 40° shows that the YSZ (111) peaks first shift to higher 2θ, then shift to lower 2θ, at last shift to higher 2θ again. The intensity of YSZ (111) peak increases with increasing the sputtering temperature, which indicates that the YSZ films become thicker with increasing the sputtering temperature.

Upon annealing, the film deposited at room temperature (about 28oC) shows a weak diffraction peak at 28.6∘, correspond to (111) Bragg peak of crystalline YSZ. The

broad feature describe to amorphous phase. As the temperature from 28oC to 500oC the peak position of the YSZ (111) shifts to higher 2θ, which is believed to origin from the tensile stresses in the YSZ films. And the stress will release gradually as the film thickness approaches to a certain value. For the film deposited at 300oC, the peak site of YSZ (111) shifts to lower 2θ compared to the film deposited at 500oC. It is suggested that the tensile stress emerges again. The second time appearance of tensile stress has been reported several times for (Re) BCO films [18, 19]. It is believed that surface roughness [20], the oxygen vacancies [21] and tilted grains [22] can be the reasons of this phenomenon. The peak site of YSZ (111) shifts to higher 2θ for the film fabricated with temperature 300oC, which indicates the decrease of tensile stress for the film.

Table 2 FWHM and grain size YSZ nanostructure

Temperature deposition	Crystallographic (HKL)	FWHM	Grain size (nm)
100°C	(111)	0.1349	20.5
200°C	(111)	0.2268	21.6
300°C	(111)	0.2133	24.2
500°C	(111)	0.1338	26.6

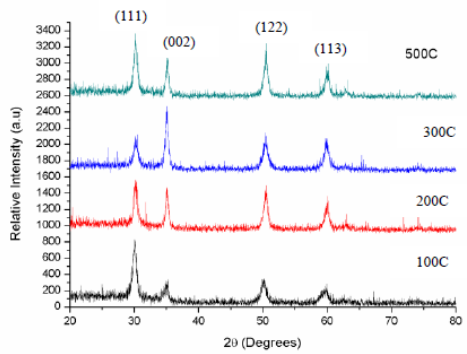

Fig. 4 XRD θ − 2θ patterns of YSZ films deposited with sputtering temperature from 28oC until 400oC from 20° to 55°.

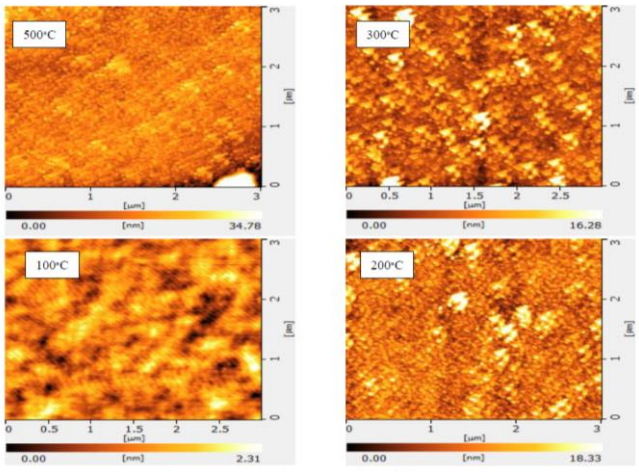

Fig. 5 AFM images of YSZ nanostructure deposited on Al2O3 at different power from 100∘C to 500∘C.

Figure 5 illustrates the AFM topography images of YSZ films deposited at 100oC to 500oC. in all cases, the nano-grain size are homogeneous distributed all over the substrate surfaces. The surface of the films deposited at 100oC is rougher than the other films deposited at higher substrate temperature. The minimum surface roughness roughness at (2.31nm) has been observed from YSZ films deposited at 100oC. A further increase in substrate temperature does not lead to any improvements in surface roughness. Instead of the surface roughness slightly increases when the substrate temperature increases. Similar AFM observation reported by Krishnan (2005).

The enhancement in surface smoothness with substrate temperature from room temperature to 500oC is attributed to the higher surface atom diffusion ((Wang *et al*., 2013). The grain growth and thus the grain sizes are proportional to the surface diffusion and increases with the substrate temperature. The increasing trend of RMS roughness with the further increase in average sizes (Chen *et al*., 2002).

4. CONCLUSION

The YSZ layers are deposited by RF sputtering. We have systematically investigated the effects of deposition parameters sputtering temperature and RF power on the developments of the texture, roughness and grain size of the YSZ films. It is found that for YSZ films high temperature deposition with 500oC favours (111)-oriented growth, while high power deposition 150W favours (022)-oriented growth. Nevertheless, the (111) orientation of YSZ film with high power 150W is a consequence of thermodynamic mechanism aiming for the lowest surface energy. The roughness and grain size of the YSZ films are greatly affected by sputtering power. Both the grain size and roughness increase as sputtering temperature increases. The mechanism of this can be explained very well by Bartelt et al's[19] theory . In addition, the emergence of a sudden increase in roughness for YSZ film deposited at a sputtering temperature of 300oC can be mainly explained by the strain relaxation mechanism. At last, high quality YSZ film have been successfully deposited on sapphire Al_2O_3 glass the optimal substrate.

ACKNOWLEDGEMENTS

This work was supported by Ministry of Science, Technology and Innovation, Malaysia through Long Term Research Grant No. 4L825.

REFERENCES

[1] An, J., Bae, J., Hong, S., Koo, B., Kim, Y. B., G??r, T. M., & Prinz, F. B, *Scripta Materialia*, *104* (2015) 45.
[2] Bernay, C. E., Ringuedé, A., Colomban, P., Lincot, D., & Cassir, M. *J. Phys. Chem. Solids*, *64*(9-10) (2003) 1761.
[3] Chen, K., L¨, Z., Ai, N., Huang, X., Zhang, Y., Xin, X., Su, W. *J. Power Sources*, *160*(1) (2006) 436.
[4] Chen, X. J., Khor, K. A., Chan, S. H., & Yu, L. G. *Mater. Sci. Eng. A*, *374*(1-2) (2004) 64.
[5] Chen, X. J., Khor, K. A., Chan, S. H., & Yu, L. G. *Mater. Sci. Eng. A*, *374*(1-2) (2004) 64.
[6] Curtin, S., Gangi, J., IEA, Tan, E. K., Materials, N., Flexcell, T., Yu, Q. *Technology Roadmap*, *22*(3) (2014) 55.

[7] de Souza, S. *Solid State Ionics*, *98*(1-2) (1997) 57.
[8] Depla, D., Besnard, A., & Lamas, J. *Vacuum*, *125* (2016) 118.
[9] Dincer, I., & Colpan, C. O. (2013). Solid Oxide Fuel Cells, 41–44.
[10] Ding, J., & Liu, J. *Solid State Ionics*, *179*(21-26) (2008) 1246.
[11] Fabbri, E., Pergolesi, D., & Traversa, E., *Sci. Technol. Adv. Mater.*, *11*(4) (2010) 044301.
[12] Feng, H., Chen, L., Xie, Z., & Sun, F. *J. Power Sources*, *286* (2015) 406.
[13] Garcia-Garcia, F. J., Yubero, F., González-Elipe, A. R., Balomenou, S. P., Tsiplakides, D., Petrakopoulou, I., & Lambert, R. M. *Int. J. Hydrogen Energy*, *40*(23) (2015) 7382.
[14] Guo, C. X., Wang, J. X., He, C. R., & Wang, W. G. *Ceram. Int. 39*(8) (2013) 9575.
[15] Halinen, M. (n.d.). *Improving the performance of solid oxide fuel cell systems*.
[16] Hidalgo, H., Reguzina, E., Millon, E., Thomann, a.-L., Mathias, J., Boulmer-Leborgne, C., Brault, P. *Surface Coatings Technol.*, *205*(19) (2011) 4495.
[17] Ikhu, D., Ahmad, W., Kawada, T., Sakai, N., Yokokawa, H., Dokiya, M., Tarancón, A. *ACS Nano*, *13*(9) (2013) 13.
[18] Jeong, H. J., Kim, J. W., Bae, K., Jung, H., & Shim, J. H., *ECS Transactions*, *57*(1) (2013) 3059.
[19] Kishimoto, H., Yashiro, K., Shimonosono, T., Brito, M. E., Yamaji, K., Horita, T. Mizusaki, J. *Electrochimica Acta*, *82* (2012) 263.